

Chapter 2

Translation of Ribozyme-Based Gene Expression Control Devices from Yeast to Mammalian Cells

Abstract

Engineered biological systems have potential applications in areas ranging from foundational biological studies to biofuel production to cellular therapeutics. Robustly operating systems require effective control mechanisms to achieve fine-tuned performance, and a variety of synthetic, RNA-based control devices capable of gene expression regulation have been demonstrated. The majority of RNA-based control devices reported thus far have been developed in bacteria and yeasts—model organisms with well-characterized tools for genetic manipulation to facilitate the rapid prototyping and optimization of new devices. However, few devices have been shown to function in higher organisms, including human cells. While bacteria and yeasts are important cellular hosts in many research and industrial processes, several important application areas—particularly those in health and medicine—require mammalian systems and compatible control devices. Therefore, the ability to transfer synthetic devices developed in model organisms to mammalian systems is critical to the versatility and practicality of such devices in downstream applications. Here, we systematically examine the translation of ribozyme-based control devices developed in the yeast *Saccharomyces cerevisiae* to gene expression regulation in the model cell line human embryonic kidney (HEK) 293. We demonstrate that the knockdown efficiency of ribozyme-based devices is lower in HEK cells by 2- to 5-fold compared to that observed in yeast, and the switch dynamic range is reduced in HEK cells due to the mammalian hosts' limited capacity to withstand ligand toxicity. We identify several tuning strategies, including thermodynamically based sequence modification and multiple-copy expression, by which regulatory stringency can be improved for applications in mammalian systems, and we demonstrate functional ON,

OFF, and AND-gate switches in HEK 293 cells. We conclude that performance tunability is a device property essential to the transportability of these genetic devices across organisms, and we further identify several system parameters—including actuator efficiency, input signal toxicity, and genomic integration—as critical to the development of ribozyme-based control systems in higher organisms.

Introduction

RNA-based control devices with diverse regulatory mechanisms have been developed in recent years¹, and the great majority of RNA devices described to date have been developed in model organisms such as the bacterium *Escherichia coli* and the yeast *Saccharomyces cerevisiae*. Relatively high growth rates and the ease of genetic manipulation enable faster device prototyping and optimization in these model hosts compared to higher organisms such as mammalian cells. However, not all regulatory mechanisms are transportable across organisms. For example, translation initiation in prokaryotes is mediated by the hybridization of the 16S rRNA to the ribosome binding site (RBS) located 6–7 nucleotides upstream of the start codon. In contrast, translation in eukaryotes is initiated through a 7-methyl guanosine cap that recruits the translation initiation machinery. Therefore, an RNA device designed to regulate translation initiation in bacteria cannot function in eukaryotic hosts and vice versa.

It follows that the versatility of RNA devices depends on the use of components that do not rely on cell-specific machinery in performing regulatory functions. Alternatively, given a defined set of applications, devices can be developed in and tailored for specific host organisms of interest. The latter construction strategy circumvents the need for broad transportability across species, but incurs the potential cost of longer development periods required for designing and optimizing devices in complex organisms. The non-trivial increase in time and resource investments, as well as the technical complexities that accompany development work in higher organisms, has contributed to the relatively small number of functional RNA devices that have been generated in mammalian cells²⁻⁴. At the same time, many important application areas—

particularly those in health and medicine—require regulatory devices that can function in higher organisms, especially human cells. Therefore, the development of devices that function independently of cell-specific machineries and the demonstration of transportability across different organisms are critical to the versatility of synthetic RNA devices.

Previous work in the Smolke Laboratory presented a framework for assembling ligand-responsive, ribozyme-based devices from modular components in the yeast *S. cerevisiae*^{5, 6} (see Chapter 1 for a detailed description). This RNA device assembly platform allows deliberate choice of the input molecule, fine-tuning of basal expression level and dynamic range, and the ability to program higher-order cellular information processing, making it uniquely suited for downstream therapeutic applications. However, the transportability of these ribozyme-based devices to gene expression control in mammalian cells remains to be demonstrated. Since the hammerhead ribozyme's cleavage-based regulatory mechanism is self-catalyzed and independent of cell-specific machinery, we hypothesized that the ribozyme switches should be functional in mammalian hosts, even though the quantitative performance levels of the devices may be affected by differences in the cellular environment. Here, we demonstrate the ability of ribozyme switches to regulate gene expression in human embryonic kidney (HEK) 293 cells. Through the process of transferring ribozyme switches from yeast to human cells, we identify performance tunability as a device property critical to transportability across organisms. Furthermore, we examine several system parameters—including ribozyme-mediated knockdown efficiency, ligand toxicity, and impact of device integration into the

host genome—that are essential to the construction of ribozyme-based gene-regulatory systems in mammalian hosts.

Results

Ribozyme Devices Show Reduced Knockdown Efficiency but Retain Ligand Responsiveness and Performance Tunability in Human Cells. We developed a model system to characterize ribozyme-based devices in mammalian cells, in which EGFP was expressed from a cytomegalovirus (CMV) promoter and ribozyme switches were inserted in the 3' UTR of the EGFP coding region. Transient transfections of the switch constructs were performed in HEK Flp-In 293 cells, and gene expression output was evaluated by EGFP intensity measured with a flow cytometer. Several theophylline- and tetracycline-responsive ON switches with distinct transmitter sequences that program different response properties (i.e., varying basal expression levels and dynamic ranges) were examined in the presence and absence of the appropriate small-molecule input. Ligand molecules were supplied at the maximum concentration that still permitted cell growth. Due to differences in ligand toxicity toward different cell types, the ligand concentration used in HEK transfections was ten-fold lower than that used in yeast characterization studies (Table 2.1)^{5,6}.

Results from transient transfection assays indicate that each of the examined devices is capable of gene expression knockdown, with L2bulge8 exhibiting the highest knockdown efficiency and lowest basal expression level. The relative knockdown efficiencies among the devices are consistent with previous characterization results in

yeast, suggesting the tuning capability of the transmitter sequences is retained in the new host organism (Table 2.1, (1x) constructs in Figure 2.1).

Table 2.1. Theophylline-responsive ribozyme switch activities in yeast and HEK cells

Switch Construct	Theophylline Input		Expression Range ^{a,b}		Switch Activity (Fold) ^c	
	Yeast	HEK	Yeast	HEK	Yeast	HEK
L2bulge1(1x)	10 mM	1 mM	40% - 89%	88% - 89%	2.23	1.01
L2bulge8(1x)			12% - 48%	62% - 73%	4.00	1.18
L2bulge9(1x)			30% - 72%	88% - 104%	2.40	1.18

^aData for yeast cells are taken from Ref. 6, Table S1; data for HEK cells are taken from the experiment reported in Figure 2.1.

^bExpression range indicates fluorescent protein expression levels in the absence (OFF state) and presence (ON state) of theophylline at the concentration indicated for each cell type.

^cSwitch activity is calculated by dividing the ON-state expression level by the OFF-state expression level and reported as a fold-change.

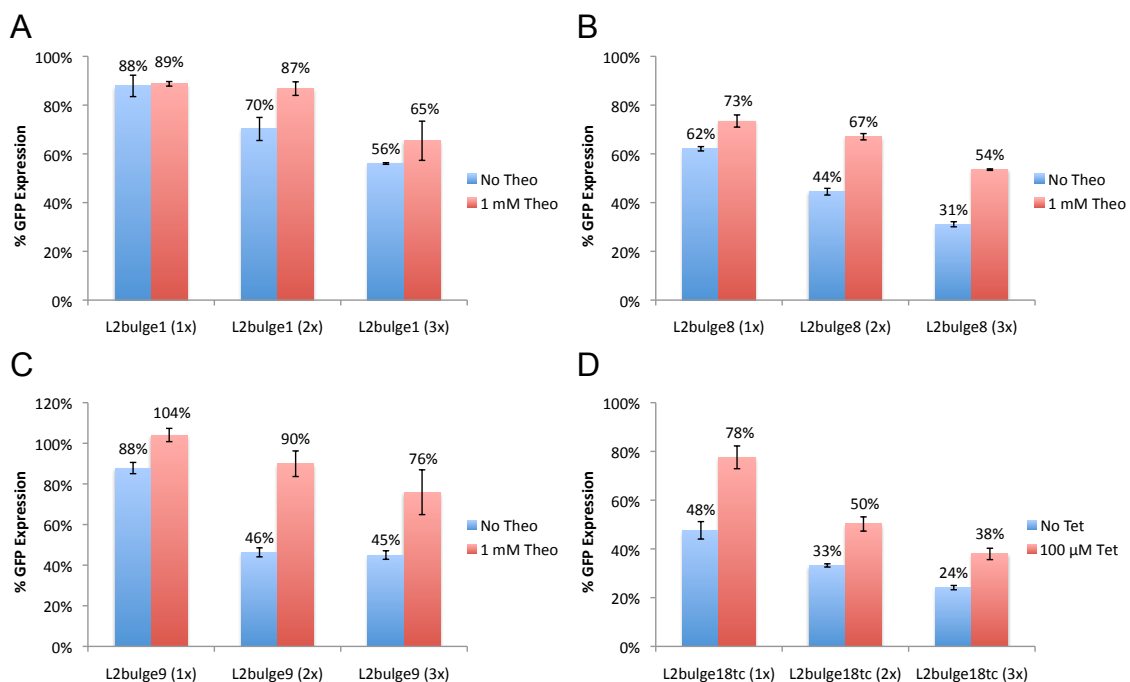


Figure 2.1. Ribozyme switches provide tunable, ligand-responsive gene regulation. GFP expression levels are reported for constructs encoding the theophylline-responsive switches (A) L2bulge1, (B) L2bulge8, and (C) L2bulge9, and the tetracycline-responsive switch (D) L2bulge18tc. Fluorescence values were normalized to those of the inactive ribozyme control cultured at corresponding ligand concentrations. Reported values are mean \pm s.d. from triplicates.

Despite their evident knockdown activities, all the devices tested show significantly higher basal expression levels (i.e., gene expression in the absence of ligand input) in HEK cells compared to those observed in yeast, and the switch dynamic ranges are more limited in HEK cells (Table 2.1). The reduced dynamic ranges may have resulted from the lower ligand concentrations used in HEK cultures. However, elevated basal expression levels suggest that cellular mechanisms associated with this gene-regulatory scheme, including ribozyme cleavage activities as well as mRNA and protein synthesis and degradation, likely occur at different rates in the two cell types. The observed reduction in ribozyme-mediated knockdown efficiency in HEK cells is consistent with previously reported data on the transcript levels of reporter genes coupled to the unmodified sTRSV hammerhead ribozyme in yeast (8%)⁵ versus HEK cells (20%)⁷. Furthermore, differences in the method of genetic manipulation (i.e., stable transformation in yeast versus transient transfection in HEK cells) may also have contributed to the different activities observed.

Multiple-Copy Expression Fine-Tunes Regulatory Stringency and Improves Switch Dynamic Range. To address the reduction in ribozyme-mediated knockdown efficiency in mammalian cells, we implemented a second tuning strategy based on linking multiple copies of ribozyme switches in the 3' UTR of the transgene. The ribozyme switches are expected to act independently in this design⁶, where only one of the switches needs to be in the ribozyme-active state to cleave and inactivate the transcript. Multiple-copy switch devices increase the probability of ribozyme-mediated transcript cleavage, thereby lowering basal expression levels. However, expressing multiple copies of the same or

similar ribozyme switches increases the potential of misfolding of the RNA elements, which would disable the devices. To maintain the structural and functional independence of each switch, we introduced standardized spacer sequences that form stable hairpin structures between each copy of the ribozyme switch (Figure 2.2). We used the RNAstructure software⁸ to verify that the most thermodynamically favorable conformation for the entire RNA sequence is one in which each switch is properly folded. Previous studies in yeast have examined the effect of expressing two copies of the ribozyme switches⁶. Given the reduced ribozyme cleavage efficiency observed in HEK cells, we anticipated the need to integrate additional copies of switch devices and devised a sequential cloning strategy to allow for the systematic integration of a theoretically unlimited number of ribozyme switches in the 3' UTR of a given gene (Figure 2.2, see Materials and Methods).

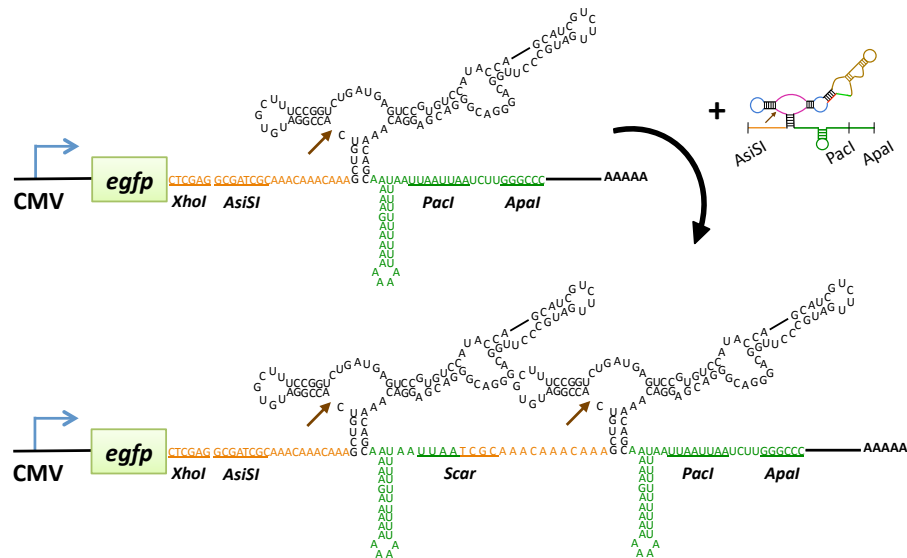


Figure 2.2. Ribozyme switch devices are modularly integrated into mammalian expression vectors. Ligand-responsive ribozyme switch devices (here depicting L2bulge1) are inserted in the 3' UTR of the transgene encoding for EGFP, which serves as a reporter protein for the evaluation of regulatory activities. A modular insertion strategy allows the implementation of multiple copies of ribozyme switches to tune regulatory stringency. The restriction sites AsiSI and PacI, which generate compatible sticky ends, allow reuse of the sites after each switch insertion. Spacer sequences (orange and green) form a stable hairpin structure that provides structural insulation and maintain the functional independence of each switch.

If the cleavage activity of each ribozyme were an independent event, the probability of the transcript remaining intact (i.e., all ribozymes remaining in the inactive state) would be the product of each ribozyme's probability of remaining uncleaved. Therefore, each additional copy of the switch would result in a fixed fold-decrease in basal expression level equivalent to the inverse of the probability of each ribozyme remaining uncleaved. The probability of a ribozyme switch remaining uncleaved can be indirectly measured by the expression levels of single-copy constructs. Therefore, each additional copy of the L2bulge1, L2bulge8, L2bulge9, and L2bulge18tc switches is expected to result in fold-decreases of 1.1-, 2.1-, 1.1-, and 1.6-fold, respectively.

Transient transfection results show that the multiple-copy switch systems lower basal expression levels while maintaining ligand-responsive switch activities (Figure 2.1). With the exception of L2bulge9, each addition copy of a ribozyme switch results in a constant fold-decrease in basal expression levels (1.3-fold for L2bulge1, 1.4-fold for L2bulge8, and 1.4-fold for L2bulge18tc), consistent with independent ribozyme activity. The actual magnitudes of change for L2bulge1 and L2bulge18tc are close to the predicted values, whereas that for L2bulge8 is not. In addition, the L2bulge9 switch exhibits a dramatic decrease in basal expression level with the first additional ribozyme copy but no further improvement with the second additional copy. These behaviors suggest that the assumption of independent cleavage activities may not be valid for all switch designs and additional factors such as cooperativity and kinetic limitations in ribozyme cleavage may be involved. It is also possible that protein expression level is not a perfect surrogate measurement for mRNA cleavage activity, thus introducing discrepancies between theoretical and actual results.

In addition to lowering the basal expression levels, multiple-copy switch systems improve the ligand-responsive dynamic range for the majority of constructs tested (Figure 2.1). Specifically, switches with the highest basal expression levels show the largest improvements in dynamic range measured both in fold change (i.e., ratio of ON-state to OFF-state expression levels) and in absolute values. L2bulge1, which has no switch activity when expressed as a single-copy construct, shows theophylline-responsive gene expression upregulation when implemented in two and three copies. L2bulge8, which has a significantly higher knockdown efficiency than L2bulge1, also exhibits increased switch dynamic range (measured in fold) with each increasing ribozyme copy number. The improvement in switch activity may be attributed to the lowered basal expression level, which effectively broadens the maximum range between the ON and the OFF states. Although the maximum ON state may not be accessible in these model systems due to HEK cells' limited tolerance for the small-molecule ligands used, the ability to increase the potential dynamic range makes multiple-copy expression a valuable tool for fine-tuning the performance of regulatory systems constructed with ribozyme-based devices.

Ribozyme Devices Exhibit Titratable Switch Activity Dependent on Basal Expression Levels. The ability to modulate output signal intensity by adjusting input signal strength is a critical property of genetic control devices. An important characteristic of the ribozyme switch devices is a dose-dependent response to input concentrations. To verify the titratable response of ribozyme switch devices in human cells, we performed transient transfections of constructs harboring ON and OFF switches

responsive to theophylline and tetracycline in HEK cells supplemented with various levels of the appropriate ligands. Results indicate titratable switch activity in the majority of devices tested, with gene expression increasing or decreasing with input concentration as prescribed by the device design (Figure 2.3). Consistent with previous observations, devices with high basal expression levels have relatively poor ligand-responsive ON switch activities (L2bulge1tc, Figure 2.3B). In addition, L2bulgeOFF1tc, a tetracycline-responsive OFF switch, exhibits weak switch activities. Yeast and HEK cells have different sensitivity levels to small-molecule ligands, and toxicity issues limit the maximum tetracycline input in HEK cultures to a concentration substantially lower than that used in yeast cultures (150 μ M and 1 mM for HEK and yeast, respectively)⁶. This difference in input signal strength is likely the main cause of the reduced switch dynamic ranges observed in HEK cells.

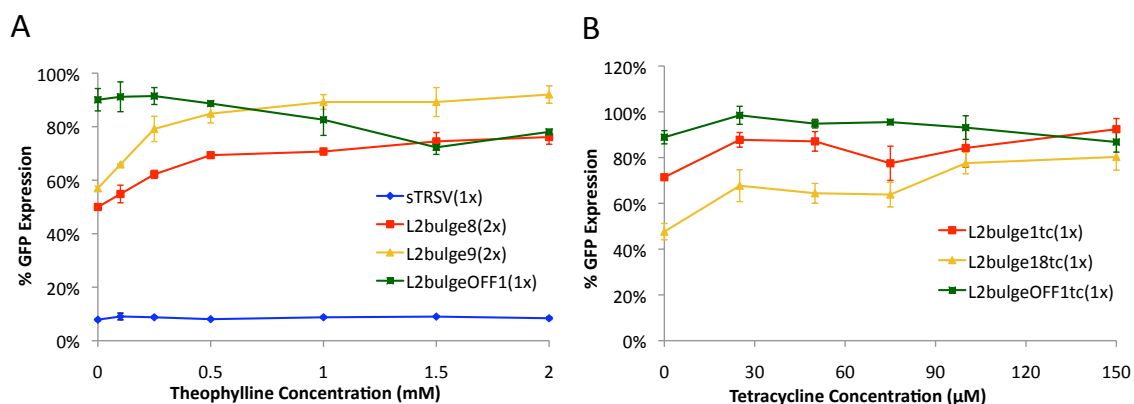


Figure 2.3. Ribozyme switches provide titratable gene regulation. GFP expression levels are reported for constructs encoding (A) theophylline- and (B) tetracycline-responsive switches. (A) L2bulge8(2x) and L2bulge9(2x), ON switches. L2bulgeOFF1(1x), an OFF switch. sTRS, a non-switch, fully active hammerhead ribozyme control. (B) L2bulge1tc(1x) and L2bulge18tc(1x), ON switches. L2bulgeOFF1tc(1x), an OFF switch. Values are reported as described in Figure 2.1.

Stable Integration of Ribozyme Devices Provides Consistent, Long-Term Regulatory Activity. The performance stability of genetic control devices is a critical system attribute in a wide range of applications, including cellular therapeutics and the industrial production of pharmaceuticals or biofuels using genetically modified cell strains. To evaluate the long-term robustness of ribozyme switch devices in mammalian cells, we performed site-specific integration of the switch devices in HEK Flp-In 293 cells. Site-specific stable integration was chosen for three main reasons. First, long-term characterization cannot be performed on transiently transfected cells, which generally lose transgene expression within one week in the absence of selection pressure due to the loss or dilution of plasmids. Any downstream application that operates for more than a few days will require stably integrated systems. Second, stably integrated cell lines have significantly more consistent gene expression levels compared to transiently transfected cultures. Transient transfections result in heterogeneous populations of cells receiving different numbers of plasmids and thus expressing the encoded transgene at vastly different levels. Stable integration permits the selection of monoclonal cultures with a tight distribution of gene expression levels, enabling more accurate quantification of system performance (Figure 2.4A). Third, site-specific integration with the Flp-In system (Invitrogen) allows direct comparison of various stably integrated cell lines harboring different constructs. Stable integration in mammalian cells can be achieved through several methods, including viral transduction and lipid-based transfection followed by selection. However, such methods generate polyclonal integrants with random insertion sites for the introduced transgene, and more than one copy of the transgene may be integrated into the genome. While it is possible to isolate monoclonal populations for

each cell line by cell sorting or limiting dilution, direct comparisons cannot be made across different cell lines due to differences in integration site and copy number, both of which affect gene expression levels. The Flp-In system generates isogenic cell lines with one copy of the transgene inserted into a specific genomic location, thus allowing accurate comparisons to be made across cell lines harboring different transgenic constructs.

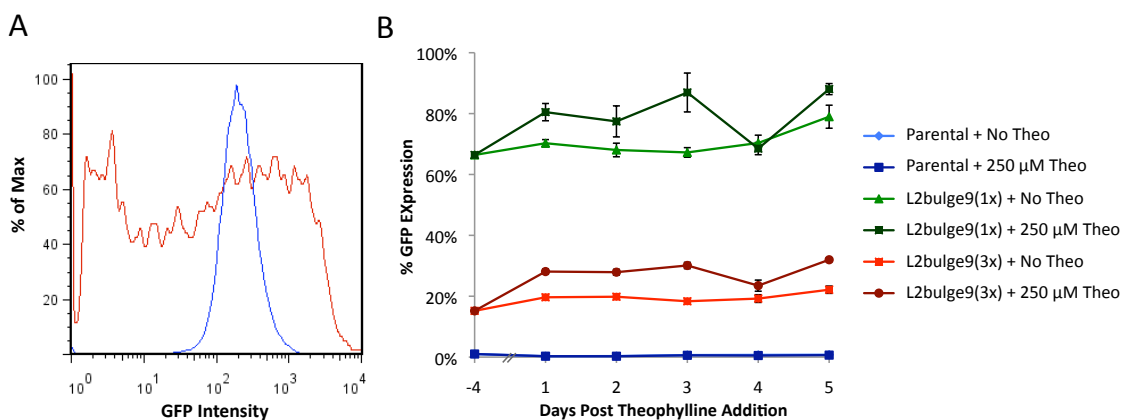


Figure 2.4. Stably integrated cell lines show tight gene expression distributions and demonstrate long-term regulatory activities by ribozyme switches. (A) Stably integrated cell lines show a substantially narrower gene expression distribution compared to transiently transfected cells. Blue, HEK cells stably integrated with a plasmid encoding EGFP coupled to an inactive ribozyme; red, HEK cells transiently transfected with the same plasmid. (B) HEK cell lines stably expressing one or three copies of the theophylline-responsive ribozyme switch L2bulge9 exhibit ligand-responsive ON switch behavior and an increase in knockdown activity with increasing ribozyme copy numbers. Stable cell lines were cultured in the presence or absence of 250 μ M theophylline for five days. The parental HEK Flp-In 293 cell line was included as a negative control. Values are reported as described in Figure 2.1.

Stable cell lines expressing one or three copies of the theophylline-responsive ON switch L2bulge9 or an inactive ribozyme (positive control) inserted in the 3' UTR of the *egfp* transgene were generated. The resultant cell lines were characterized for ligand-responsive gene regulatory activities by culturing in the presence or absence of 250 μ M theophylline for five days, and the parental HEK Flp-In 293 cell line was included as a negative control. The theophylline concentration used with the stable cell lines was four-

fold lower than that used in transient transfection studies because HEK cells cannot withstand long-term exposure to the higher theophylline concentration. Despite the lowered input concentration, gene expression results indicate theophylline-responsive ON switch activities and an increase in knockdown efficiency with increasing ribozyme copy numbers (Figure 2.4B). Gene expression reached steady-state levels within 24 hours and remained stable through the five-day time-course, supporting a rapid and robust response to the molecular input. Compared to transient transfection results, the stably integrated cell lines show substantially lower basal expression levels and slightly smaller dynamic ranges in response to ligand addition (Table 2.2). The reduced input concentration used in the time-course study is likely a major contributing factor to the decrease in dynamic range. In addition, the substantially different distribution of gene expression levels in transiently transfected samples versus stably integrated cell lines may account for the differences in basal expression levels and dynamic ranges. Specifically, the measured performance of transiently transfected samples reflects the average of heterogeneous cell populations with widely varying expression levels (Figure 2.4A). Measurements made on stably integrated cells, which are isogenic and show a tight distribution of expression levels, are likely to be more accurate reflections of device performance.

Table 2.2. Theophylline-responsive ribozyme switch activities in transiently transfected and stably integrated HEK 293 cells

Switch Construct	Theophylline Input		Expression Range ^{a,b}		Switch Activity (Fold) ^c	
	Transient	Stable	Transient	Stable	Transient	Stable
L2bulge9(1x)	1 mM	250 μ M	88% - 104%	71% - 80%	1.18	1.13
L2bulge9(3x)			45% - 76%	20% - 28%	1.69	1.43

^aData for transient transfection are taken from the experiment reported in Figure 2.1C; data for stable integration are taken from the experiment reported in Figure 2.4B, with expression levels reported as the average (arithmetic mean) of data points gathered over the five-day time-course study.

^bExpression range shows fluorescent protein expression levels in the absence (OFF state) and presence (ON state) of theophylline at the concentration indicated for each experiment type.

^cSwitch activity is calculated by dividing the ON-state expression level by the OFF-state expression level and reported as a fold change.

Translation of Higher-Order Information Processing Devices from Yeast to Mammalian Cells Requires Finely Tuned Designs with Strong Regulatory Performance. Ribozyme-based devices capable of higher-order computation have been demonstrated in yeast cells ⁶. To examine the portability of these multi-input devices in mammalian cells, we tested logic-gate devices generated by the combinatorial expression of ON switches responsive to theophylline or tetracycline (Figure 2.5A). Transient transfection results for two AND-gate devices in HEK cells suggest that robust multi-input device activity is dependent on a low basal expression level (Figure 2.5B), consistent with results observed with single-input devices (Figures 2.1, 2.3). Specifically, single-input switches capable of lower basal expression levels and larger dynamic ranges when acting as individual devices (L2bulge8 and L2bulge18tc) can be combined to build AND-gate devices with better performance levels compared to devices composed of single-input switches with higher basal expression levels and narrower dynamic ranges (L2bulge1 and L2bulge1tc). These results suggest that optimized multi-input RNA devices capable of higher-order computation in mammalian cells may be constructed by lowering the basal expression levels of both individual, single-input devices and the

combined ensemble. This could be achieved by reprogramming the transmitter sequence, implementing multiple copies of switch devices, or stably integrating the control devices into the host genome (Figure 2.1, Table 2.2). Furthermore, the use of non-toxic molecular inputs would permit the administration of higher ligand concentrations and enable access to the full switch dynamic range of each control device, which is likely much larger than what is currently achievable in HEK cells based on comparisons against results observed in yeasts.

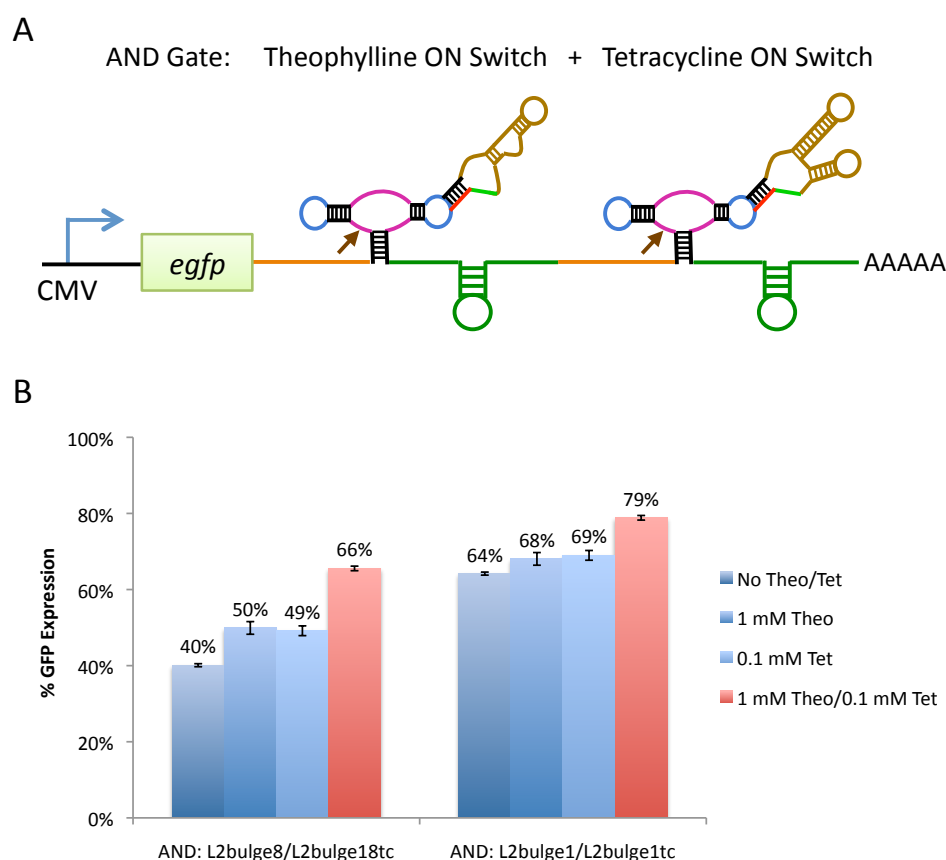


Figure 2.5. Higher-order information-processing devices must be composed of switch components with robust individual performance levels to achieve the prescribed regulatory activity in mammalian cells. (A) AND-gate devices are constructed by the tandem expression of two ON switches responsive to different input molecules. An AND-gate device comprised of theophylline-responsive and tetracycline-responsive ON switches is illustrated. (B) The combination of individual devices with strong regulatory activities enables more effective higher-order information-processing devices. Two devices were examined in HEK Flp-In 293 cells. The first AND gate consists of the L2bulge8 and L2bulge18tc switches inserted in tandem behind the *egfp* gene using the platform described in Figure 2.2. The second AND gate consists of L2bulge1 and L2bulge1tc inserted in tandem. Values are reported as described in Figure 2.1.

Discussion

RNA-based control devices incorporating a variety of regulatory strategies have been developed, mostly in bacteria and yeasts^{1, 2, 9}. However, the translation of these devices to higher organisms has been limited due to the incorporation of regulatory mechanisms that require cell-specific machinery. Important application areas such as cell-based therapies and the production of highly glycosylated pharmaceuticals require the use of mammalian systems and compatible control devices. Although a number of RNA-based control devices have been developed directly in mammalian cells^{4, 10, 11}, important advantages such as high growth rates and the relative ease of genetic manipulations make simpler model organisms, such as *S. cerevisiae*, the preferred hosts for device development. Therefore, the ability to prototype and optimize control devices in simpler organisms and later transport them to more complex cellular systems is highly desirable.

Ausländer et al. recently reported a ribozyme-based OFF switch for gene expression regulation in mammalian cells (Auslander et al.). The theophylline-responsive ribozyme was originally generated through library screening in *E. coli*. Although the switch sequence optimized in bacteria proved functional in mammalian cells, its ligand responsiveness required re-optimization through both rational design and sequence randomization and screening once implemented in the mammalian system. Furthermore, the gene regulatory strategy required fundamental changes when moving from the bacterial system to the mammalian system. Specifically, gene expression regulation in bacteria was achieved by controlling the availability of the Shine-Dalgarno sequence (Wieland and Hartig 2008b), whereas expression control in mammalian cells acted

through mRNA degradation following ribozyme cleavage in the 5' UTR of the target transcript (Auslander et al.). As a result, the device designed as an ON switch in bacteria can only function as an OFF switch in mammalian cells, and the design platform (which is dependent on library screening) does not allow for systematic alterations to reprogram and tune regulatory performance. It is also unclear whether this earlier design can support the construction of multi-input devices capable of higher-order information processing. These results highlight the importance and challenge of designing regulatory devices that are fully translatable across organisms and allow for the implementation of diverse information processing functions.

In the present work, we have demonstrated the translation of ribozyme switch devices previously developed in the yeast *S. cerevisiae* to gene expression regulation in the human cell line HEK 293. We implemented theophylline- and tetracycline-responsive ribozyme switch devices without modification in a mammalian expression system, in which the CMV promoter drives the expression of the reporter gene *egfp* with ribozyme switches inserted in the 3' UTR of the gene. Our characterization results show that the switch devices are capable of gene expression knockdown in HEK cells, exhibiting titratable activities in response to varying ligand input concentrations. However, the knockdown efficiency and switch dynamic range of any given device are generally lower in HEK cells compared to yeast cells. For certain switches, the reduction in knockdown and switch activities is sufficient to render the device largely ineffective. Although the cleavage mechanism that underpins the ribozyme-based regulatory framework is self-catalyzed and independent of cell-specific machinery, the cellular environment in which the ribozyme switches function is expected to influence their activities. Therefore, design

adjustments must be made to realize the full regulatory capabilities of ribozyme-based devices in mammalian cells, and our findings highlight performance tunability as critical to achieving device transportability across organisms.

The ribozyme-based control platform has the unique property of being modularly composed and thus amenable to a variety of performance-tuning strategies, including modifications to the transmitter sequence of individual devices and the expression of multiple ribozyme switches coupled to the same genetic target⁵. Our results show that these strategies are both transportable and essential to achieving effective regulatory activities in mammalian systems. Transmitter sequence modification was employed in the design of the theophylline-responsive ON switches L2bulge8 and L2bulge9 based on L2bulge1. While all three switches are capable of substantial knockdown and ligand-responsive switch activities in yeast, only the modified switches L2bulge8 and L2bulge9 are able to achieve knockdown and switching when expressed as single-copy constructs in mammalian cells. As a second tuning strategy, the implementation of multiple copies of a switch within a single genetic target was shown to lower basal expression levels and increase ligand-responsive dynamic ranges. While reduced ribozyme-mediated knockdown efficiency in mammalian cells can abrogate the switch activity of some devices implemented in single copies (e.g., L2bulge1 (1x), Figure 2.1), multiple-copy switch systems improve knockdown efficiency and restore ligand-responsive activity by increasing the overall probability of transcript cleavage. These results highlight the importance of modularity and tunability in the translation of control devices across organisms, and demonstrate that the ribozyme-switch platform, originally developed in yeast, possesses the required properties for effective function in mammalian hosts.

Although the fine-tuned ribozyme switches are functional in mammalian cells, several system parameters show significant differences between yeast and mammalian cells and should inform future designs of ribozyme-based regulatory systems for mammalian applications. First, our results show that the knockdown efficiency of the sTRSV hammerhead ribozyme is substantially lower in mammalian cells than in yeast. This reduced efficiency leads to a higher basal expression level (or greater “leakiness” in expression) and a smaller dynamic range. Therefore, when prototyping and optimizing devices in yeast cells, it is important to make allowances for this expected decrease in cleavage activity upon transfer to mammalian cells. Furthermore, the previously discussed tuning strategies will likely be necessary in refining the system design upon transferring into mammalian hosts. Finally, these results suggest that highly active ribozymes are necessary for the generation of ribozyme-based control devices that can function effectively in mammalian cells.

Second, different cell types have different sensitivities toward the small-molecule inputs used to regulate the RNA devices. Our results suggest that mammalian cells tend to be more susceptible to ligand toxicity compared to yeast cells. In the ribozyme switch platform, ligand binding dictates the ribozyme cleavage rate by influencing the relative stability of alternative ribozyme conformations. The cleavage rate in turn regulates the target gene expression level and the functional output of the regulatory device. Higher ligand concentrations have greater impacts on the ribozyme switch’s conformational change and expand the potential dynamic range of the device. Conversely, toxicity-imposed limitations on input concentrations set constraints on switch activities and the overall performance of the regulatory system. Therefore, even if the model organism used

for device prototyping is able to withstand high input concentrations, the destination organism's tolerance for the ligand molecules must be determined early and applied to the device development process to ensure functionality in the application of interest. Furthermore, these results indicate that sensor components (i.e., aptamers) with high affinity to ligand molecules that exhibit low cellular toxicity are critical to the utility and portability of RNA-based regulatory devices.

Third, the performance of RNA-based devices can vary dramatically depending on whether the devices are transiently or stably expressed in the mammalian host. While characterization studies are more efficiently and thus frequently performed by transient transfection, stable genomic integration is required for applications in which a narrow distribution of expression levels and long-term functionality are important. Our results show that ribozyme switches have greater knockdown efficiencies but slightly smaller dynamic ranges in stably integrated cell lines compared to transiently transfected cultures. The reduced dynamic range is likely due to the limited ligand concentration that can be tolerated for long periods by cell cultures, thus highlighting a system constraint imposed by the aforementioned issue of input toxicity.

To our knowledge, this work presents the first successful translation of an RNA-based control device from the model organism *S. cerevisiae* to gene expression control in mammalian cells. We demonstrated that ribozyme-based devices retain their designed functions when transported from yeast to human cells, and that performance tunability is a critical system attribute that permits portability across diverse organisms. Several system parameters—including actuator efficiency, ligand toxicity, and genetic integration of regulatory devices—must be considered and properly specified to achieve robust and

effective regulatory activity. These findings provide the foundation for the design and construction of ribozyme-based T-cell proliferation control systems presented in the following chapters.

Materials and Methods

Plasmid construction. All plasmids were constructed using standard molecular biology techniques¹⁴. All oligonucleotides were synthesized by Integrated DNA Technologies and all constructs were sequence verified (Laragen). Cloning enzymes, including restriction enzymes and T4 DNA ligase, were obtained from New England Biolabs, and DNA polymerases were obtained from Stratagene. The coding region of EGFP was inserted into the restriction sites KpnI and XhoI in pcDNA3.1(+) (Invitrogen). A CMV promoter and the coding region of dsRed-Express were also inserted into the plasmid to serve as transfection control. Ribozyme switch sequences were inserted into XhoI/ApaI behind EGFP, and the resulting plasmids were digested with KpnI and ApaI to obtain the EGFP-ribozyme switch sequence insert, which was then cloned into KpnI/ApaI in pcDNA5/FRT (Invitrogen).

A standardized cloning method was developed to allow for the sequential insertion of engineered ribozyme switches and corresponding control constructs in the 3' UTR of the target transgenes (Figure 2.2). The engineered ribozyme switch constructs were generated by PCR amplification using the forward primer Rz XhoI-AsiSI5' (5'AATACTCGAG GCGATCGCAAACAACAAA), where the underlined sequences indicate restriction sites for XhoI and AsiSI, respectively, and the reverse primer Rz ApaI-PacI3' (5'AATA GGGCCCAAGATTAATTAAAAAAAAAATTTTTATTTTTCTTTT

TGCTGTT), where the underlined sequences indicate restriction sites for ApaI and PacI, respectively. The italicized sequences indicate spacers flanking each ribozyme switch, and the 3' spacer sequence forms a hairpin structure consisting of A-U pairs to provide insulation for each ribozyme switch. The first copy of an engineered ribozyme switch in each plasmid was inserted via the unique restriction sites XbaI and ApaI. All subsequent copies of the engineered ribozyme switches were inserted behind the 3' end of the previous copy of ribozyme switch by digesting the plasmid with PacI and ApaI and the insert with AsiSI and ApaI, where digestions with PacI and AsiSI resulted in identical sticky ends. The resulting ligation product retained unique PacI and ApaI sites while eliminating the AsiSI site, thus allowing the cloning strategy to be repeated for each additional copy of the ribozyme switch inserted into the construct.

Ribozyme switch sequences are listed below. Color schemes: Purple, catalytic core of the ribozyme or actuator component; blue, loop region of the actuator component; brown, aptamer or sensor component; green and red, strands that participate in the competitive hybridization event; italicized, spacer sequences; underlined, restriction sites.

sTRSV hammerhead ribozyme

5'CTCGAG*AAACAAACAAAGCTG***TC**ACCGGAT**GTGCTT**TCCGGT**CTGATGAGTCC**
GTGAGGACG*AAACAGCAAAAAGAAAAATAAAAAATTTTTTGGAA* TCTAGA

Inactive ribozyme

5'CTCGAGGCGATCGC*AAACAAACAAAGCTG***TC**ACCGGAT**GTGCTT**TCCGGT**AC**
GTGAGGTCCGTG*AGGACAGAACAGCAAAAAGAAAAATAAAAAATTTTTTTTTTAAT*
TAATCTTGGGCC

L2bulge

5'CTCGAGGCGATCGC*AAACAAACAAAGCTG***TC**ACCGGAT**GTGCTT**TCCGGT**CT**
GATGAGTCCGTG*TCCATACCAGCATCGTCTTGATGCCCTGGCAGGGACGGG*
ACG*AGGACG***AAACAGCAAAAAGAAAAATAAAAAATTTTTTTTTTAATTAATCTTGG**
GCCC

L2bulge8

5'CTCGAGGCGATCGCAAACAACAAAGCTGTCACCGGATGTGCTTTCCGGTCT
 GATGAGTCCGTTGTCCATACCAGCATCGTCTTGATGCCCTTGGCAGGGACGG
 GACGGAAGGACGAAACAGCAAAAAGAAAAATAAAAAATTTTTTTTTTAATTAATCTT
 GGGCCC

L2bulge9

5'CTCGAGGCGATCGCAAACAACAAAGCTGTCACCGGATGTGCTTTCCGGTCT
 GATGAGTCCGTTGTCCAATACCAGCATCGTCTTGATGCCCTTGGCAGTGGATG
 GGGACGGAGGACGAAACAGCAAAAAGAAAAATAAAAAATTTTTTTTTTAATTAATC
 TTGGGCCC

L2bulge1tc

5'CTCGAGGCGATCGCAAACAACAAAGCTGTCACCGGATGTGCTTTCCGGTCT
 GATGAGTCCGTTGTCCAAAACATACCAGATTTTCGATCTGGAGAGGTGAAGAAT
 TCGACCACCTGGACGGACGAGGACGAAACAGCAAAAAGAAAAATAAAAAATTA
 ATTAATCTTGGGCCC

L2bulge18tc

5'CTCGAGGCGATCGCAAACAACAAAGCTGTCACCGGATGTGCTTTCCGGTCT
 GATGAGTCCGTTGTCCAAAACATACCAGATTTTCGATCTGGAGAGGTGAAGAA
 TTCGACCACCTGGACGAGGACGGAGGACGAAACAGCAAAAAGAAAAATAAAAA
 TTAATTAATCTTGGGCCC

L2bulgeOFF1

5'CTCGAGGCGATCGCAAACAACAAAGCTGTCACCGGATGTGCTTTCCGGTCT
 GATGAGTCCGTTGTTGCTGATACCAGCATCGTCTTGATGCCCTTGGCAGCAGTG
 GACGAGGACGAAACAGCAAAAAGAAAAATAAAAAATTTTTTTTTTAATTAATCTTG
 GGCCC

L2bulgeOFF1tc

55'CTCGAGGCGATCGCAAACAACAAAGCTGTCACCGGATGTGCTTTCCGGTCT
 GATGAGTCCGTTGTTGAGGAAAACATACCAGATTTTCGATCTGGAGAGGTGAA
 GAATTCGACCACCTCCTTATGGGAGGACGAAACAGCAAAAAGAAAAATAAAAAAT
 TTTTTTTT TTAATTAATCTT GGGCCC

AND: L2bulge8/L2bulge18tc

5'CTCGAGGCGATCGCAAACAACAAAGCTGTCACCGGATGTGCTTTCCGGTCT
 GATGAGTCCGTTGTCCATACCAGCATCGTCTTGATGCCCTTGGCAGGGACGG
 GACGGAAGGACGAAACAGCAAAAAGAAAAATAAAAAATTTTTTTTTTAATCGCAAAC
 AAACAACAAAGCTGTCACCGGATGTGCTTTCCGGTCTGATGAGTCCGTTGTCCAAA
 ACATACCAGATTTTCGATCTGGAGAGGTGAAGAATTCGACCACCTGGACGAGG
 ACGGAGGACGAAACAGCAAAAAGAAAAATAAAAAATTAATTAATCTTGGGCCC

AND: L2bulge1/L2bulge1tc

5'CTCGAGGCGATCGCAAACAACAAAGCTGTCACCGGATGTGCTTTCCGGTCT

GATGAGTCCGTGTCCATACCAGCATCGTCTTGATGCCCTTGGCAGGGACGGG
 ACGAGGACGAAACAGCAAAAAGAAAAATAAAAAATTTTTTTTTTAATCGCAAACAA
 CAAAGCTGTCACCGGATGTGCTTTCCGGTCTGATGAGTCCGTGTCCAAAACAT
 ACCAGATTTTCGATCTGGAGAGGTGAAGAATTCGACCACCTGGACGGGACGAG
 GACGAAACAGCAAAAAGAAAAATAAAAAATTAATTAATCTTGGGCC

NOR: L2bulgeOFF1/L2bulgeOFF1tc

5'CTCGAGGCGATCGCAAACAAACAAAGCTGTCACCGGATGTGCTTTCCGGTCT
 GATGAGTCCGTGTTGCTGATACCAGCATCGTCTTGATGCCCTTGGCAGCAGTG
 GACGAGGACGAAACAGCAAAAAGAAAAATAAAAAATTTTTTTTTTAATCGCAAACA
 AACAAAGCTGTCACCGGATGTGCTTTCCGGTCTGATGAGTCCGTGTTGAGGA
 AACATAACCAGATTTTCGATCTGGAGAGGTGAAGAATTCGACCACCTCCTTAT
 GGGAGGACGAAACAGCAAAAAGAAAAATAAAAAATTTTTTTTTTAATTAATCTTGG
 GCCC

Cell lines and cell culture maintenance. Parental HEK Flp-In 293 cells (Invitrogen) were cultured in D-MEM media (Gibco) supplemented with 10% FBS and 0.1 mg/ml zeocin (Invitrogen). Cells were seeded at 0.05×10^6 cells/ml and passaged regularly. HEK cells stably integrated with Flp-In constructs were cultured similarly, except the culture media were supplemented with 0.1 mg/ml hygromycin B (Invitrogen) and no zeocin.

Transient transfection and fluorescence quantification. All transient transfections were performed using FuGENE 6 (Roche) following the manufacturer's protocols. Cells were seeded at 0.05×10^6 cells/ml, 500 μ l/well, in 24-well plates 24 hours prior to transfection. Each transfection sample received 250 ng of plasmid DNA at a FuGENE:DNA ratio of 4:1. Fluorescence data were obtained 48 hours after transfection using a Quanta Cell Lab Flow Cytometer equipped with a 488-nm laser (Beckman Coulter). Viability was gated by side scatter and electronic volume, and viable cells were further gated for dsRed-Express expression, which served as a transfection control. EGFP

and dsRed-Express were measured through 525/30-nm band-pass and 610-nm long-pass filters, respectively. Flow cytometry data were analyzed using FlowJo (Tree Star). Geometric mean fluorescence values were normalized to those of the inactive ribozyme control cultured at the same input concentration of the appropriate ligand molecule. Mean values from triplicate samples were reported with an error range of ± 1 standard deviation.

Stable HEK Flp-In cell line generation. Six wells in a six-well plate containing 2 ml/well of parental HEK Flp-In 293 cells seeded at 0.05×10^6 cells/ml were transfected with FuGENE 6 and cultured in media without antibiotics for 48 hours. Cultures were then passaged into media containing 0.2 mg/ml hygromycin B. Cells were continuously cultured in hygromycin-containing media without passaging for 9 more days. Colonies were pooled together into one well of a six-well plate on day 11 after transfection. Cells were passaged 2 days after pooling and passaged regularly thereafter into media containing 0.1 mg/ml hygromycin B. Construct integration was verified by EGFP detection through fluorescence microscopy and flow cytometry.

Theophylline response assay for stable HEK Flp-In cell lines. Stably integrated HEK cell lines as well as the parental HEK Flp-In 293 cell line were each used to seed 30 wells in 24-well plates with 500 μ l of culture per well. Wells were seeded at different densities to allow assaying at different time points through the 5-day time-course study. Twelve wells were seeded at 0.1×10^6 cells/ml, another 12 wells were seeded at 0.05×10^6 cells/ml, and the remaining 6 wells were seeded at 0.02×10^6 cells/ml. At each seeding

density, half of the wells were fed with 250 μ M final concentration of theophylline dissolved in water and sterile-filtered with a 0.22 μ M syringe filter. Every 24 hours after seeding, 6 wells (3 with and 3 without theophylline) were analyzed by flow cytometry, starting with the wells seeded at the highest cell density. Data analyses were performed as described for transient transfections.

Acknowledgments

We thank S. Culler for generating the HEK Flp-In 293 stable cell lines. This work was supported by the City of Hope's National Cancer Institute–Cancer Center Support Grant, the National Science Foundation (fellowship to Y.Y.C.), the Alfred P. Sloan Foundation (fellowship to C.D.S.), and the National Institutes of Health (grant to C.D.S., RC1GM091298).

References

1. Win, M.N., Liang, J.C. & Smolke, C.D. Frameworks for programming biological function through RNA parts and devices. *Chem Biol* **16**, 298-310 (2009).
2. Isaacs, F.J., Dwyer, D.J. & Collins, J.J. RNA synthetic biology. *Nat Biotechnol* **24**, 545-554 (2006).
3. Yen, L. et al. Exogenous control of mammalian gene expression through modulation of RNA self-cleavage. *Nature* **431**, 471-476 (2004).
4. Yen, L., Magnier, M., Weissleder, R., Stockwell, B.R. & Mulligan, R.C. Identification of inhibitors of ribozyme self-cleavage in mammalian cells via high-throughput screening of chemical libraries. *RNA* **12**, 797-806 (2006).

5. Win, M.N. & Smolke, C.D. A modular and extensible RNA-based gene-regulatory platform for engineering cellular function. *Proc Natl Acad Sci U S A* **104**, 14283-14288 (2007).
6. Win, M.N. & Smolke, C.D. Higher-order cellular information processing with synthetic RNA devices. *Science* **322**, 456-460 (2008).
7. Khvorova, A., Lescoute, A., Westhof, E. & Jayasena, S.D. Sequence elements outside the hammerhead ribozyme catalytic core enable intracellular activity. *Nat Struct Biol* **10**, 708-712 (2003).
8. Mathews, D.H. et al. Incorporating chemical modification constraints into a dynamic programming algorithm for prediction of RNA secondary structure. *Proc Natl Acad Sci U S A* **101**, 7287-7292 (2004).
9. Wieland, M. & Hartig, J.S. Artificial riboswitches: synthetic mRNA-based regulators of gene expression. *ChemBiochem* **9**, 1873-1878 (2008).
10. An, C.I., Trinh, V.B. & Yokobayashi, Y. Artificial control of gene expression in mammalian cells by modulating RNA interference through aptamer-small molecule interaction. *RNA* **12**, 710-716 (2006).
11. Beisel, C.L., Bayer, T.S., Hoff, K.G. & Smolke, C.D. Model-guided design of ligand-regulated RNAi for programmable control of gene expression. *Mol Syst Biol* **4**, 224 (2008).
12. Auslander, S., Ketzer, P. & Hartig, J.S. A ligand-dependent hammerhead ribozyme switch for controlling mammalian gene expression. *Mol Biosyst* **6**, 807-814.

13. Wieland, M. & Hartig, J.S. Improved aptazyme design and in vivo screening enable riboswitching in bacteria. *Angew Chem Int Ed Engl* **47**, 2604-2607 (2008).
14. Sambrook, J. & Russell, D.W. *Molecular Cloning: A Laboratory Manual*, Edn. 3. (Cold Spring Harbor Press, Cold Spring Harbor; 2001).